Title

Contrasting Root System Architecture Development and Response to High Temperature in an *Aegilops tauschii*-Derived Wheat Line and its Recurrent Parent

Sultan Md Monwarul Islam[1], Izzat Sidahmed Ali Tahir[2,3], and Kinya Akashi [1,3,4] *

1 United Graduate School of Agricultural Sciences, Tottori University, 4-101 Koyama-Cho-Minami, Tottori City, Tottori Prefecture, 680-0945, Japan; smmonwar051@gmail.com
2 Wheat Research Program, Agricultural Research Corporation, Wad Medani P.O. Box 126, Sudan; izzatahir1@gmail.com
3 International Platform for Dryland Research and Education, Tottori University, 1390 Hamasaka, Tottori City, Tottori Prefecture, 680-0001, Japan; izzatahir1@gmail.com
4 Faculty of Agriculture, Tottori University, 4-101 Koama-Chou-Minami, Tottori City, Tottori Prefecture, 680-0945, Japan; akashi.kinya@tottori-u.ac.jp
* Correspondence: akashi.kinya@tottori-u.ac.jp; Tel: (+81) 857 31 5352

Abstract:

Multiple Synthetic Derivatives (MSD) is a unique hexaploid wheat population that captures *Aegilops tauschii* diversity and exhibits broad variation in agronomic traits. However, root system architecture (RSA), a key determinant of productivity and environmental adaptation, has been little studied in this population. Here, we used MSD417 as an example genotype to establish a systematic framework for root trait analyses in the MSD. A two-dimensional cultivation system was developed to obtain daily RSA images of wheat seedlings grown on calico cloth. Root growth and high-temperature stress responses of MSD417 were then compared to those of its recurrent parent, Norin 61 (N61). Under controlled temperature, MSD417 showed significantly higher total root length, root system width, and convex hull area than N61, indicating vigorous juvenile root growth. MSD417 also exhibited a wider angle between the outermost seminal roots, facilitating horizontal soil exploration while maintaining a rooting depth comparable to N61. In contrast, high-temperature suppressed root growth and obscured most genotypic differences. Microscopic analysis revealed a lower height-to-width ratio of coleorhiza tissue in MSD417 under control condition, suggesting restricted downward expansion. These results demonstrate the usefulness of this approach and provides the first step in analyzing RSA in the genetically diverse MSD and similar populations.

Keywords: wheat; Multiple Synthetic Derivative; Norin 61; MSD417; high temperature stress; arid region; seminal root angle; coleorhiza.

1. Introduction

Wheat (*Triticum aestivum* L.) holds major agricultural importance as a staple food for a large portion of the global population, accounting for 18% of total dietary calories globally **[1]**. Climate change is expected to threaten wheat production, resulting in an estimated 16% reduction over the next three decades, particularly in the tropical regions of Africa and Southern Asia, where wheat is consumed daily as a staple food **[2]**. Wheat is highly sensitive to temperatures above the optimum range, and global wheat yield could drop by 6% for each degree-Celsius temperature rise **[3,4]**.

Root system architecture (RSA) refers to the set of traits (e.g., root length, number, angle, and distribution along the soil profile) used to characterize the structural features of the root system **[5,6]**. RSA is influenced by a combination of internal (e.g., underlying genetics and developmental influences) and external factors such as environmental causes (e.g., climate, physical and chemical properties of the soils, and biotic influence), leading to genotype-by-environment interactions that greatly affect root system architecture **[6,7]**. The plastic nature of the root system and its development allow plants to adapt to changing environments **[6]**, and it has been proposed as an important breeding target for a 'second green revolution' for the development of climate-resilient crops **[8,9]**.

Multiple Synthetic Derivatives (MSD) is a unique population of synthetic wheat that harbored a large genetic variation in *Aegilops tauschii* in a background of hexaploid wheat **[10–13]**. The MSD population was initially developed by crossing and backcrossing 43 different primary synthetic wheat lines with the Japanese wheat cultivar 'Norin 61' (N61). Successive self-pollination of the population up to BC_1F_5 generation resulted in the development of representative genotypes collectively called the MSD panel **[11,12]**. The genotypes in the MSD population show diverse morphology, agronomic traits, and their environmental responses, including heat, drought, and low soil nutrients such as nitrogen and phosphorus **[10,12,13]**. Based on the high field performance in Sudan, one of the hottest wheat-growing areas in the world, five selected MSDs genotypes (MSD296, MSD34, MSD392, MSD417, and MSD54) were further analyzed for their physiological and molecular responses to high temperature in a controlled environment, revealing that the diversity in the agronomic traits was associated with distinct molecular responses **[14]**. Among these genotypes, MSD417 exhibited one of the highest performances across various traits, including fertility, thousand-kernel weight, harvest index, and yield. These findings suggest that the MSD population is a useful genetic material for future breeding programs. However, features of the root structures and their environmental responses have not been examined to date.

Evaluating RSA traits is often challenging because access to the root is limited, typically requiring laborious, costly, and time-consuming procedures, which constrain phenotypic analysis. Nevertheless, fully exploiting variability in RSA traits could yield substantial benefits **[5,15–18]**. In-field measurements of the root system tend to be destructive **[17]**, thus mostly undertaken at a single time-point for an individual plant, and are often labor-intensive or capture only a portion of the RSA. RSA measurements in controlled conditions typically lead to more reproducible phenotypic results **[19]**. Various analytical platforms have been used to assess RSA in soil-based research conducted in controlled environments, including rhizoboxes made of wood, glass plates, metal boxes, and transparent polyvinyl chloride tubes **[20–22]**. On the other hand,

non-soil-based systems, such as transparent pots **[23]**, germination paper **[24]**, agar plates **[25]**, GLO-Roots **[26]**, GrowScreen-Rhizo **[27]**, and paper or cloth pouches **[28,29]** enable non-invasive time-course analyses of root development and easier root sampling. However, these systems often require investment in specialized devices. In the present study, we developed a simple and cost-effective two-dimensional platform for RSA analysis and used it to evaluate MSD417, a candidate model for heat-tolerant wheat genotypes in the MSD population.

2. Materials and Methods

2.1 Plant material

Seeds of bread wheat cultivar 'Norin 61' (hereafter referred to as N61), and MSD genotype MSD417 were kindly provided by Prof. Hiroyuki Tanaka (Faculty of Agriculture, Tottori University, Tottori, Japan) and Dr Yasir Serag Alnor Gorafi (Arid Land Research Center, Tottori University, Tottori, Japan), respectively. The seeds were multiplied in pots at a greenhouse facility in the Faculty of Agriculture, Tottori University, Tottori, Japan, and fully mature seeds were harvested in 2024 and used for the experiments.

2.2. Construction of the root growth panel

Wheat plants were grown on a custom-made, two-dimensional root growth panel based on the protocols described by **[28,29]** with the following modification. First, two sheets of paper towel (Kimtowel, a four-layer pulp, unbleached, Nippon Paper Crecia, Tokyo, Japan) were cut into 34 cm in height and 30 cm in width by scissors, then the bottom corners of both sides were trimmed off to remove rectangles measuring 3 cm in height and 3 cm in width (Figure 1A). The paper towels were soaked in a 2000-fold diluted HYPONeX nutrient solution (Hyponex Japan, Osaka, Japan) and then placed on the surface of an acrylic board (31 cm height, 30 cm width, and 0.5 cm thickness) to extend 3 cm below the bottom edge of the acrylic board. A 33 cm × 30 cm sheet of black calico cloth was laid on top of the paper towel. The cloth and paper towel were attached to the acrylic board by wrapping them with three 1 mm-wide No. 18 rubber bands (Daiso Industries, Higashi-Hiroshima, Hiroshima, Japan) horizontally, 2 cm below the top edge of the acrylic board (Figure 1B). To prevent moisture on the surface of the calico cloth from evaporating, a high-density polyethylene sheet (L-501-2, 0.05 mm thickness, As One, Osaka, Japan) was cut into a 31 × 30 cm square and placed over the cloth. This allowed roots to grow between the polyethylene sheet and the calico cloth; the latter served as a supporting substance for root growth. To prevent light exposure to the roots, a second black calico cloth measuring 33 × 30 cm was placed over the polyethylene sheet, extending up to 2 cm above the top edge of the acrylic board. The 2-cm protruding part of the cloth was folded over the top of the acrylic board to prevent light from entering the stack, while the center of the folded cloth was cut out to create a 3-cm-wide window for shoot emergence. Four 3-cm-wide binding clips were placed at the corners of the board to secure the entire system (Figure 1C). Hereafter, this system is referred to as the root growth panel.

To accommodate the root growth panels in a growth chamber, two pieces of wood (48 cm in length, 4 cm width, and 3 cm in height) were placed along the inner bottom of a plastic tray (50 cm in length, 35 cm in width, and 20 cm in height) (Figure 1C), and filled with the 2000 folds-diluted HYPONeX solution to a depth of 3 cm. The 18 panels were stacked vertically on top of the woods in the tray (Figure 1D), ensuring that the paper towels protruding downward from the panels were submerged in the solution. Finally, the whole unit, including the growth panels, was covered (except the upper middle part of the growth panels) with the same calico cloth (45 cm ×

45 cm), followed by a high-density polyethylene sheet (45 cm × 45 cm) to protect water evaporation from the growth panels. The unit was placed in a growth chamber (14/10 h light/dark regime, 22 °C/18 °C day/night temperatures, light intensity of approximately 350 μmol m^{-2} s^{-1}, and relative humidity of 50-60%).

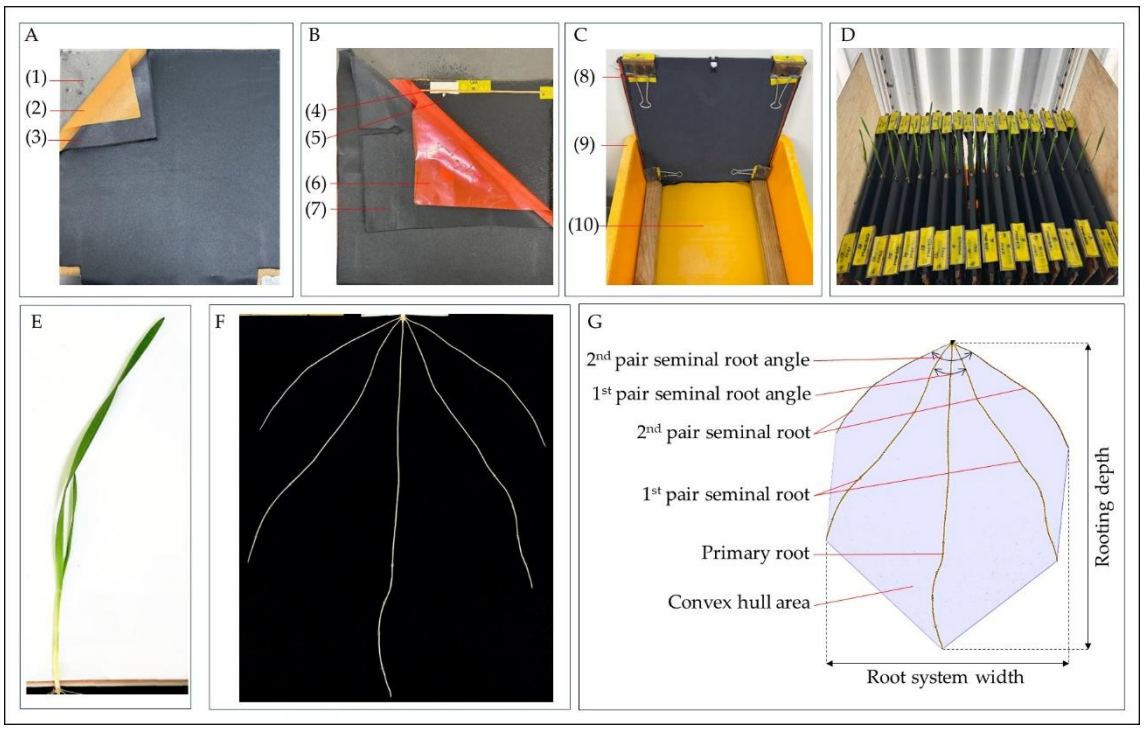

Figure 1. Two-dimensional root growth panel for analysing root system architecture. (A) A stack on the back side of the panel composed of an acrylic board (1), sheets of a kimtowel (2), and a black calico cloth (3). (B) A placement and further stacking onto the back side stack by rubber bands that secured the seed (4), a pre-germinated seed (5), a polyethylene sheet (6), and a second black calico cloth (7). (C) Installation into the container. The stacked panel was secured at four corners with clips (8) and placed in a plastic tray (9) that was filled with the nutrient-mixed water solution (10). (D) The vertically stacked panels in a growth chamber. (E) A photograph of a representative MSD417 shoot at day 8 under control conditions. (F) A representative image of root growth of N61 at day 8 under high-temperature conditions. (G) An image of root tracing by ImageJ plugins with SmartRoot and its root traits.

2.3. Plant growth conditions

The seeds were placed on top of two 85 mm-diameter filter papers (Filter paper type-2, Advantec, Tokyo, Japan) in a 90 mm-diameter petri dish and imbibed with 10 ml of tap water. Another piece of the same filter paper was used to cover the seeds. The petri dish was capped with a transparent lid, wrapped with aluminum foil, and incubated at 4 °C for two days. The petri dish was incubated at 25 °C in the dark for another day. The uniformly germinated 12 seeds of each genotype were placed at the central position of the rubber band in the root growth panels and covered by two pieces of filter paper (3 cm × 2 cm), which were moisturized in advance with a 2000-fold HYPONeX solution to prevent the seeds from drying (Figure 1B). The panels were incubated under normal temperature conditions (14/10 h light/dark regimes, 22 °C/18 °C

day/night temperatures). After four days, half of the panels were transferred to a high-temperature chamber with day/night temperatures of 42 °C/18 °C for an additional four days, while the control plants were maintained at normal temperature conditions (22 °C/18 °C).

2.4. Root imaging and biomass measurement

To visualize the root system architecture, the polyethylene sheets and light-blocking black calico cloth were removed from the root growth panel, and the root systems and shoot morphology were photographed using a bench-top photograph system (model ET16 Plus, CZUR Tech, Shenzen, China). After taking root image, the 2000-fold HYPONeX solution was evenly sprayed onto the roots, followed by reassembling the supporting black calico cloth and the panels for further growth. This image acquisition was performed daily. On the eighth day, the root and shoot were harvested separately, weighed on an electric balance to record fresh weight, and then dried for three days in a drying oven at 80 °C to record their dry weight.

2.5. Root image processing and statistical analysis

All root images were processed using ImageJ (version 1.54g) plugins with SmartRoot (Version 4.21) **[30]**. Rooting depth, root system width, individual root length, seminal root angle, and shoot height were measured. Data were analyzed and visualized in the R statistical environment (version 4.5.0, R Core Team, 2025) using a set of custom-made R scripts deposited in Supplementary Document S1. Tukey's method was applied for multiple comparisons.

Table 1. Traits measured in the root growth panels

Traits	Abbreviation	Unit	Note
Rooting depth	RD	cm	Vertical length from root base to root tip
Shoot height	SH	cm	Length between the shoot base and tip
Root dry weight	RDW	mg	
Shoot dry weight	SDW	mg	
Root-to-shoot ratio	RSR		Root dry weight / shoot dry weight
Total root length	TRL	cm	Total length of all seminal roots and the primary root
Specific root length	SRL	cm mg^{-1}	Total root length/root dry weight
Primary root length	PRL	cm	Length of primary root
First pair seminal root length	FPSRL	cm	Mean length of the first two seminal roots
Second pair seminal root length	SPSRL	cm	Mean length of the third and fourth seminal roots
First pair seminal root angle	FPSRA	degree	Angle between the first two seminal roots
Second pair seminal root angle	SPSRA	degree	Angle between the third and fourth seminal roots
Root system width	RSW	cm	Maximum horizontal spread of the root system
Convex hull area	CHA	cm^2	A convex polygon drawn to enclose all the outermost points of the roots.

3. Results

3.1. Root biomass allocation and root system architecture

The germinated wheat plantlets were grown in root growth panels under controlled conditions (22/18 °C day/night) for four days. Then, half of the plantlets were transferred to a high-temperature growth chamber with day/night temperatures of 42/18 °C for an additional four

days to undergo high-temperature treatment. In N61, the primary roots reached approximately two-thirds of the growth panel depth in eight days, accompanied by typically four seminal roots, with a primary root extending diagonally downward (Figure 2A). High temperature resulted in the growth inhibition for both the primary and the seminal roots in N61 (Figure 2B). MSD417 showed a similar pattern for root growth, but a tendency toward longer roots and a broader root system width was observed (Figure 2C, D).

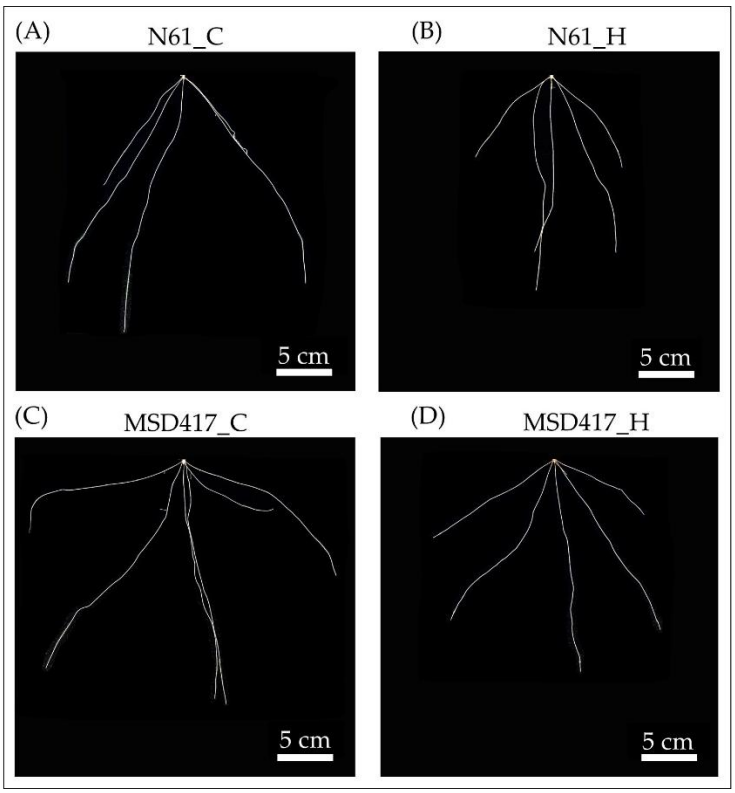

Figure 2. Representative images of N61 and MSD417 in contrasting temperature conditions at day eight. (A) N61_C- N61 in control condition, (B) N61_H- N61 in high-temperature condition, (C) MSD417_C- MSD417 in control condition, and (D) MSD417_H- MSD417 in high-temperature condition.

To evaluate root system characteristics quantitatively, trait parameters were measured as defined in Table 1 and Figure 1G. Root dry weight (RDW) differed significantly among genotypes and treatment conditions (Figure 3A). Under control conditions, MSD417 exhibited significantly higher RDW than N61, both under control and high-temperature conditions, as well as its RDW under high-temperature conditions. In contrast, no statistical difference in shoot dry weight (SDW) was observed between genotypes or temperature conditions (Figure 3B). Consequently, the root-to-shoot ratio (RSR) was the highest in the MSD417 under control conditions (mean value of 0.81) compared to the other genotype/condition combinations (mean values in the range of 0.62–0.67) (Figure 3C), suggesting that the MSD417 genotype possesses a preferential allocation of biomass to the root system under non-stress conditions.

Despite these differences in biomass allocation, traits such as rooting depth (RD) and shoot height (SH) did not differ significantly between the two genotypes after eight days (Figure 3D, E). This indicated that the genotypic differences in root traits were not associated with vertical soil exploration. Under high-temperature conditions, both genotypes showed significant

reductions in various traits. For instance, the RD was significantly affected by high temperature in both genotypes, resulting in 26% and 24% reductions in N61 and MSD417, respectively, compared with the control conditions (Figure 3D). Since no genotypic differences in RD were observed, subsequent analyses focused on geometric parameters describing the spatial configuration and distribution of the root system.

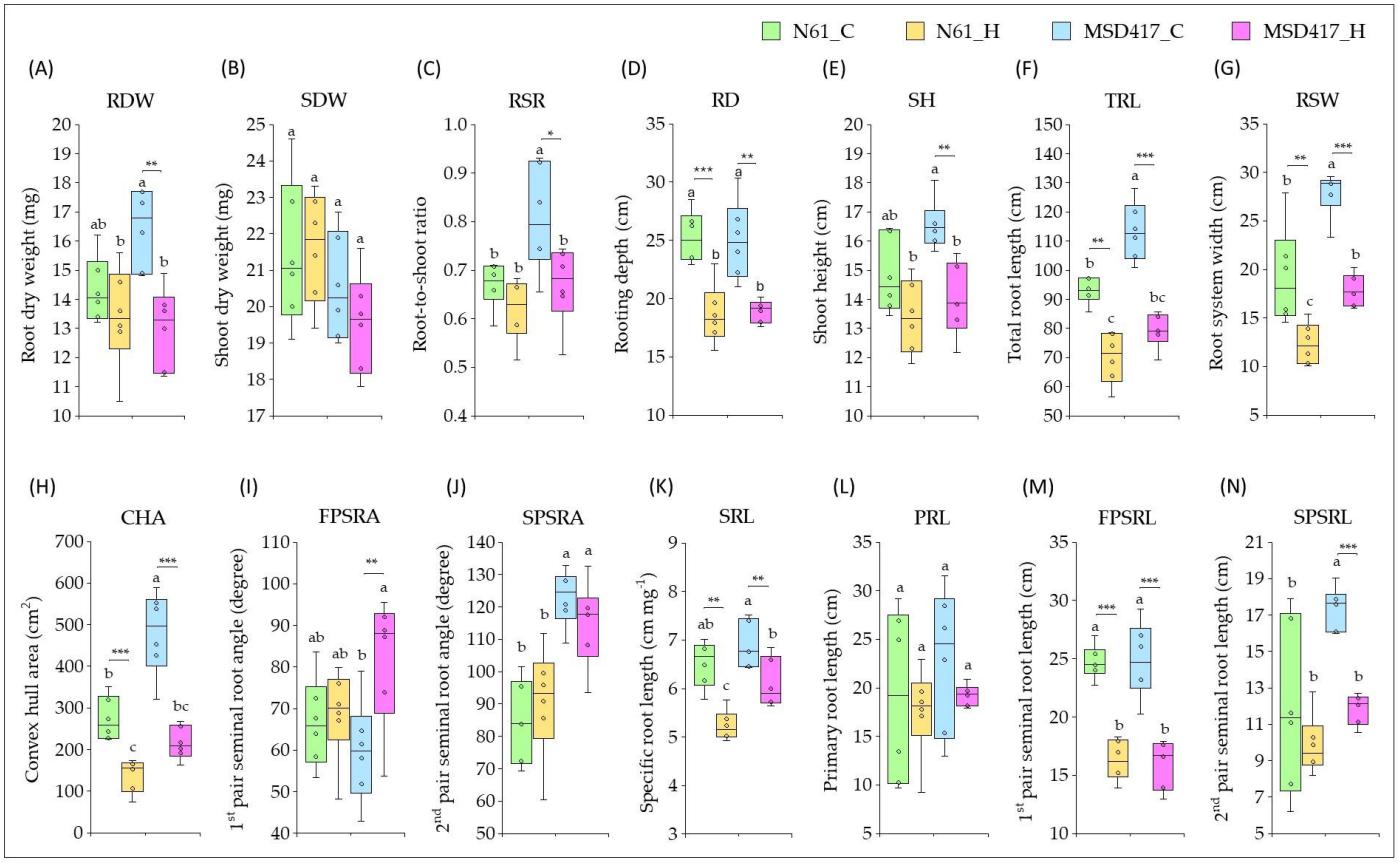

Figure 3. Variation in root and shoot morphological traits in contrasting temperatures of N61 and MSD417. The legend at the top of the panels shows four genotype-by-environment combinations: N61_C, N61_H, MSD417_C, and MSD417_H, representing N61 in the control condition, N61 in the high-temperature condition, MSD417 in the control condition, and MSD417 in the high-temperature condition, respectively. (A) root dry weight, (B) shoot dry weight, (C) root-to-shoot ratio, (D) rooting depth, (E) shoot height, (F) total root length, (G) root system width, (H) convex hull area, (I) first pair seminal root angle, (J) second pair seminal root angle, (K) specific root length, (L) primary root length, (M) first pair seminal root length, and (N) second pair seminal root length. Data for N61 and MSD417 were compared using Tukey's HSD post hoc test; different letters indicate significant differences among genotypes under contrasting temperature conditions. Data for the same genotypes raised under contrasting temperature conditions were compared using Student's t-test ($p < 0.05$, $p < 0.01$, $p < 0.001$; $n = 6$). Abbreviations of the trait parameters are shown in Table 1.

3.2 Geometric configuration of the root system

To further characterize root system architecture, geometric traits describing root length distribution and spatial expansion were analyzed. Under the control condition, total root length

(TRL) was longer in MSD417 (113.25 ± 9.12 cm) than in N61 (93.02 ± 3.98 cm), while high temperature decreased the TRL in both genotypes (Figure 3F). Root system width (RSW) and convex hull area (CHA) were also significantly larger in MSD417 (Figure 3G, H), indicating enhanced horizontal expansion in MSD417. Notably, while the angle between the first pair of seminal roots did not differ significantly between the two genotypes (Figure 3I), the angle between the second, outermost pair of seminal roots was larger in MSD417 (122.96 ± 7.85 and 114.91 ± 11.92 degree under control and high temperature conditions, respectively), in comparison to those of N61 (84.39 ± 11.46 and 90.72 ± 15.79 degree, respectively) (Figure 3J), suggesting that the wider root system in MSD417 is at least partly attributable to the increased divergence of the outermost seminal roots.

3.3 Contribution of the individual root components:

Specific root length (SRL) showed no significant change under the control conditions of N61 and MSD417 (Figure 3K); however, SRL decreased significantly under the high-temperature conditions for both genotypes. Primary root length (PRL) did not differ significantly among conditions or genotypes (Figure 3L), and the length of the first pair seminal root (FPSRL) was significantly shorter under the high-temperature conditions for both genotypes (Figure 3M). In contrast, the length of the second pair seminal root (SPSRL), corresponding to the outermost seminal roots, was significantly greater for the MSD417 under the control conditions (17.37 ± 1.06 cm) than for N61 (11.89 ± 4.30 and 9.84 ± 1.48 cm under control and high-temperature conditions, respectively), and MSD417 high-temperature conditions (11.85 ± 0.77 cm) (Figure 3N), highlighting the uniqueness of this trait in MSD417 genotype.

3.4 Temporal dynamics of seminal root development:

Time course analysis further confirmed the architectural divergence between the two genotypes. The elongation of PRL and FPSRL did not differ significantly between the N61 and MSD417 genotypes under either control or high-temperature conditions (Figure 4A, B). By contrast, SPSRL was consistently greater in the MSD417 under the control conditions throughout the examined period compared to the control of N61 and the high-temperature conditions of both genotypes (Figure 4C), suggesting that early vigorous development of the outermost seminal roots during the seedling stage is a defining characteristic of the MSD417 genotype.

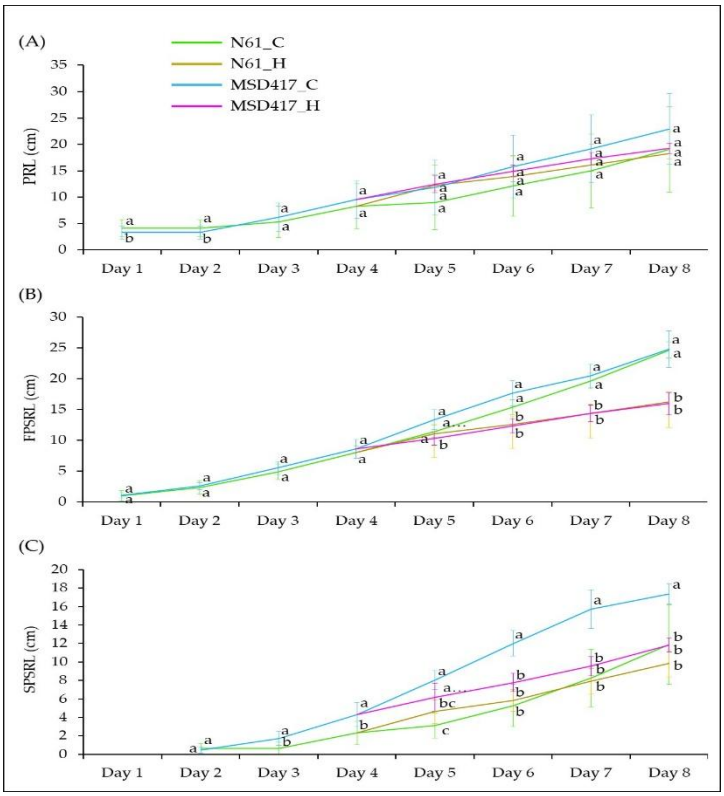

Figure 4. Line graphs showing the variation in the development of different root traits of N61 and MSD417 over different days after germination in contrasting temperatures. (A) primary root length, (B) 1st pair seminal root length, and (C) 2nd pair seminal root length. The legend at the top of the panels shows four genotype-by-environment combinations: N61_C, N61_H, MSD417_C, and MSD417_H, representing N61 in the control condition, N61 in the high-temperature condition, MSD417 in the control condition, and MSD417 in the high-temperature condition, respectively. PRL- primary root length, FPSRL- 1st pair seminal root length, and SPSRL- 2nd pair seminal root length. Data for the N61 and MSD417 were compared using Tukey's HSD post hoc test; different letters denote significant differences among genotypes under contrasting temperature conditions (n = 6).

3.5. Multivariate structure of root system architecture

To visualize relationships among traits and to gain insight into the main sources of variation among genotypes under contrasting temperatures, principal component analysis (PCA) was performed (Figure 5). The first two principal components (PC1 and PC2) collectively explained 73.6% of the total variance, with PC1 accounting for 52.6% and PC2 for 21.0%. The PCA scores

largely separated the control and high-temperature conditions along PC1, with the control plants of both genotypes clustered on the positive side, whereas the high-temperature-stressed plants were positioned on the negative side. Separation of genotypes was also observed: plants in the MSD417 control condition clustered in the higher PC1 region, while those in N61 tended to cluster near the origin or scattered toward the PC2-negative plane. Under high-temperature conditions, MSD417 tended to cluster in the PC2-positive region, whereas N61 showed a tendency toward lower PC2 values.

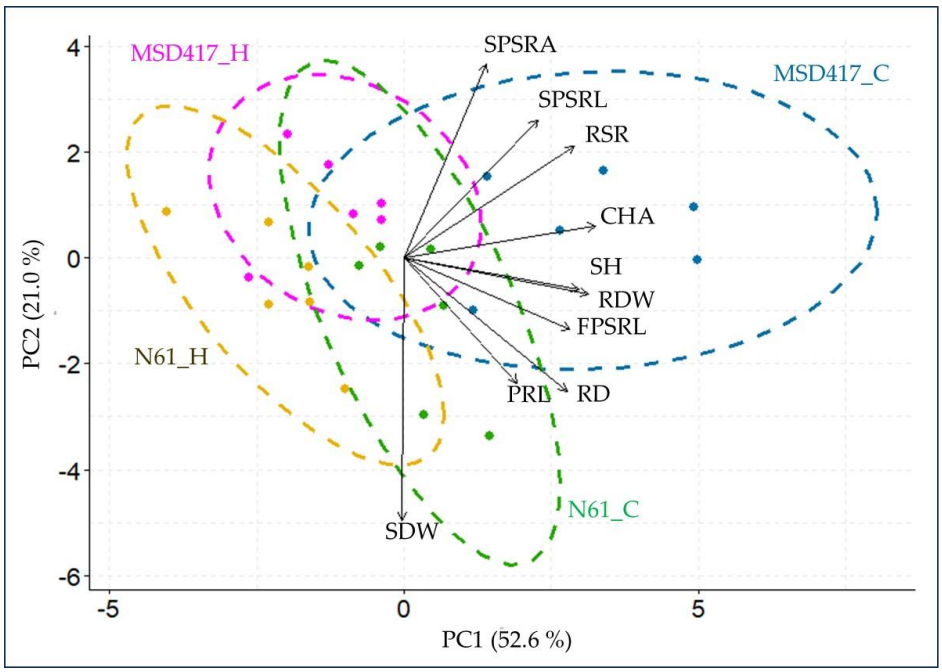

Figure 5. Principal component analysis (PCA) biplot of different traits of N61 and MSD417 in the contrasting temperature conditions. Colored dots represent the scores of plant individuals (n = 6) for N61 in the control condition (N61_C), N61 in the high-temperature condition (N61_H), MSD417 in the control condition (MSD417_C), and MSD417 in the high-temperature condition (MSD417_H), respectively. Vectors in black color indicate directions and strength of the loadings of the trait parameters as shown in Table 1.

The loading vectors showed that most traits had strong positive loadings on PC1, suggesting that these traits were strongly associated with the control condition and were inhibited under the high-temperature condition (Figure 5). Interestingly, SPSRA and SPSRL had higher PC2 values than the other parameters, suggesting that the larger angle and length of the second pair seminal roots (SPSRL) are associated with MSD417 genotypes. It was also found that RSR and CHA were associated with the MSD417 under control conditions, suggesting a trend toward a higher root-to-shoot ratio and a larger root convex hull area in this genotype. By contrast, the loading of SDW showed a strongly negative PC2 value (Figure 5), consistent with the trend of higher shoot dry weight in N61 compared to MSD417 (Figure 3B).

3.6. Root traits correlations of the two genotypes at different temperatures

To examine relationships among root parameters, correlations were calculated for each genotype-temperature condition combination (Figure 6). In the N61 genotype under the control

condition, many trait parameter combinations showed positive correlations, including RD with RDW, SDW, and RSW; SH with SDW, PRL, and RSW (Figure 6A). However, SPSRL, SRL, RSR, and RSW showed negative correlations with several other root traits, including SH and SDW. On the other hand, under the high-temperature condition N61, while the majority of trait pairs correlated positively, SPSRA remained inversely correlated with most traits, and SRL showed negative correlations with RSR and RD (Figure 6B). In the MSD417 genotype, distinct trends in parameter correlations were observed compared with N61. Under the control condition, SDW showed negative correlations with RDW, RSR, SH, and SPSRL (Figure 6C). In contrast, under the high-temperature condition, new sets of strong negative correlations were observed, including SRL with RDW, RSR, and SH, as well as SDW with SPSRA (Figure 6D).

High temperature induced significant shifts in trait correlations across both genotypes (Figure 6). In N61, correlations involving SPSRA shifted from positive to strongly negative, while those involving SPSRL reversed from strongly negative to positive. A similar trend occurred in MSD417, where the correlation between RDW and SDW weakened significantly under high-temperature conditions, as the relationships of SRL with RDW, RSR, and SH, and that of SDW with SPSRA changed to strong negative correlations. Despite these shifts, certain relationships remained stable across all genotype-temperature condition combinations: CHA and RSW maintained a consistent positive correlation, whereas SRL consistently showed a negative correlation with RDW.

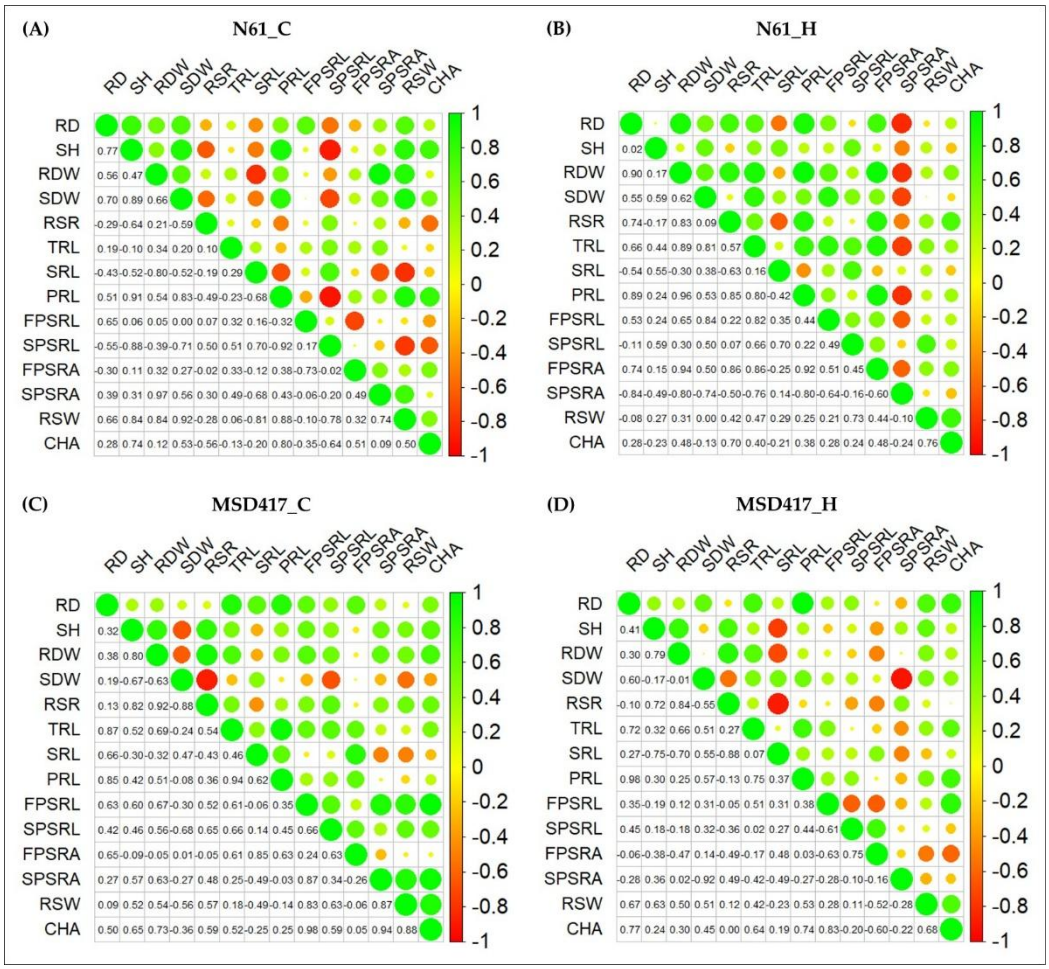

Figure 6. Positive correlation (in green) and negative correlation (in red) among different root and shoot traits. N61 in (A) control condition, and (B) high-temperature condition; and MSD417 in (C) control condition, and (D) high-temperature condition, n= 6. Abbreviations of the trait parameters are shown in Table 1.

3.7. Topology of the seminal root emergence

Analysis of root traits of the MSD417 described above suggested that this genotype has a larger angle of the outermost seminal roots, as indicated by the higher SPSRA value (Figure 3I). To examine how this trait relates to seed morphogenesis during germination, the root emergence pattern from seeds was compared microscopically (Figure 7). At seven days after germination, a massive clump of coleorhiza cells was observed at the base of the primary and other seminal roots in both genotypes (Figure 7A, B). Depth of the initiation point of the outermost seminal root, estimated by calculating the distance between the intersection point of the perpendicular line from the center of the root initiation point and the root axis, and the boundary line between stem-root tissue, was statistically indistinguishable between N61 and MSD417 (Figure 7C, D, E). However, N61 developed a coleorhiza tissue that extended vertically downward, unlike MSD417, forming a larger, lob-like structure (Figure 7A, F). Consequently, MSD417 had a smaller height-to-width ratio of coleorhiza tissue compared to N61 (Figure 7G), suggesting a suppression of coleorhiza tissue expansion in the downward direction in MSD417.

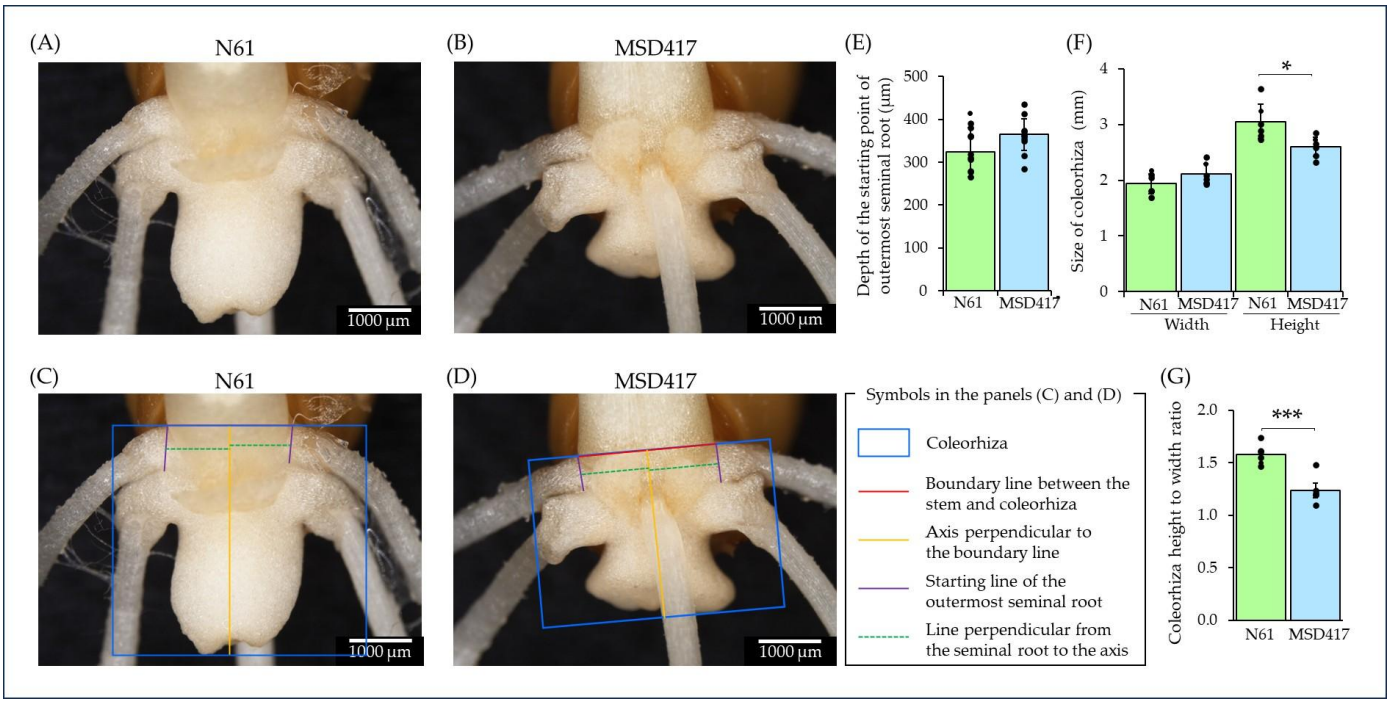

Figure 7. Microscopic representative images of N61 (A) and MSD417 (B) at 7 days after germination, grown in the control condition. Measuring technique of coleorhiza and depth of the starting point of the outermost seminal root of N61 (C), and MSD417 (D). Bar graph showing the depth of the starting point of the outermost seminal root (E), size of the coleorhiza (F), and coleorhiza height to width ratio of N61 and MSD417 at 7 days after germination (G). Data for each genotype were compared using Student's t-test ($p < 0.05$, ***$p < 0.001$); n = 6.

4. Discussion

In this study, using a 2D-root phenotyping platform, we successfully characterized the *Aegilops tauschii*-derived MSD417 genotype as exhibiting a distinct root system architecture compared to its recurrent parent, N61, under controlled, high-temperature conditions. Under control conditions, MSD417 developed a larger root system, characterized by a wider angle of the outermost roots and a unique transverse expansion of the coleorhiza; the latter feature may suggest novel cell wall remodeling mechanisms, as discussed below. These results revealed that introgression from *Aegilops tauschii* into the MSD417 genotype resulted in distinct modifications in root system architecture, rather than changes in overall biomass accumulation or rooting depth. Despite the limitations imposed by high temperatures, the higher specific root length of MSD417 indicates an inherited advantage in resource acquisition.

Root system architecture (RSA) is one of the primary factors influencing crop productivity, significantly impacting global food supply through water use efficiency, soil nutrient uptake, and other agronomic traits **[6,8]**. Developing climate-resilient wheat genotypes that are better adapted to the challenges of climate change requires understanding how introgression alters RSA without compromising above-ground growth. Although wheat MSD population showed a wide variation for various agronomic traits, including grain yield, biomass, heading time, stress tolerance, resource use efficiency, and nutritional contents and composition **[12,31–34]**their RSA characteristics have been poorly described.

Under the control condition, MSD417 exhibited a higher root-to-shoot ratio (RSR) and total root length (TRL) compared to N61, indicating that MSD417 allocated more resources to root growth (Figure 3C, F). Although rooting depth (RD) was not different between the two genotypes, the second pair of seminal root length (SPSRL) and root system width (RSW) were significantly larger in MSD417 than in N61, resulting in the larger convex hull area (CHA) in MSD417 (Figure 3D, N, G, H). The larger RSW in MSD417 was also observed under high-temperature conditions (Figure 3G), suggesting that MSD417 may possess a trait characterized by enhanced lateral root growth. The larger angle of the outermost, second pair of seminal roots and the vigorous growth of these seminal roots during the juvenile stage suggested that the broader root system of MSD417 is at least partially attributable to the more lateral growth characteristics of the outermost seminal roots (Figure 3J, N). The larger angle and enhanced growth of the second pair of seminal roots were also indicated by PCA biplot as prominent traits of MSD417 (Figure 5). A diversity in the angle of the second pair of seminal roots has been reported in wheat cultivars grown in agar and soil systems **[35]**.

In many crops, the root angle significantly affects the efficiency of acquiring water and nutrients from different soil layers **[36]**. Deep root systems are considered superior at acquiring mobile nutrients such as water and nitrogen. On the other hand, shallow root systems formed by the horizontally expanded roots are thought to be advantageous for absorbing phosphorus, which has low mobility and tends to accumulate near the topsoil, as well as for adapting to waterlogging by obtaining oxygen for root respiration **[37]**. The lateral root elongation is thought to involve the competing gravitropic and antigravitropic offset mechanisms **[36]**. A complex gene network has been proposed for gravity perception, signal transduction, and root morphological responses. For example, studies in molecular genetics and cellular biology showed that the actin-binding protein Rice Morphology Determinant (RMD) mediates the interaction between actin filaments and gravity-sensing organelles (statoliths) in rice roots, thereby regulating root growth

angle in response to soil phosphate availability **[38]**. In other studies, rice mutants of DEEPER ROOTING 1 (*DRO1*) and the quantitative trait locus SOIL SURFACE ROOTING 1 (*qSOR1*), the homologues of LAZY genes responsible for root gravity sensing in Arabidopsis, exhibited reduced root gravitropism and resulted in a shallower root angle **[39–41]**. Therefore, the enhanced lateral root elongation observed in MSD417 in the present study suggests that this genotype may possess distinct genetic factors for root gravity sensing, signal transduction, or response mechanisms compared with its recurrent parent, N61.

In crop plants, a tradeoff between the allocation of root biomass near the soil surface and deep exploration has been discussed **[16]**. In the present study, it is noteworthy that MSD417 showed a larger RSW without reducing RD (Figure 3G, D), resulting in a larger CHA than N61 (Figure 3H). It has been suggested that CHA is an indicator for soil exploration to capture below-ground resources **[42,43]**. Enhanced biomass production and yield in MSD417 were reported in a previous study **[14]**. Further studies are needed to investigate the field performance of MSD417, including its ability to acquire water and nutrients from the underground, and its impact on yield.

This study showed that root growth of both MSD417 and N61 genotypes was markedly inhibited upon exposure to acute heat stress at a daytime temperature of 42 °C for four days (Figure 3). No significant genotypic differences were found in most RSA parameters, such as root length and biomass, suggesting that the responses of both genotypes to high-temperature stress were largely similar, at least during the juvenile stage. Extremely high temperature stress has been known to inhibit root growth and significantly affect root system architecture **[44–48]**. The cellular and molecular processes underlying heat-induced growth inhibition include decreased cellular membrane integrity in roots **[49–51]**, denaturation of cellular proteins and nucleic acids **[52,53]**, increased production of reactive oxygen species and lipid peroxidation products **[54]**, decreased translocation of photoassimilates from the above ground tissues **[55]**, leading to synergistically reduced rates of cell division and elongation in the root tissues **[48,56,57]**. The current study applied acute heat stress, which may have had determinant effects on RSA and obscured genotypic differences. Future studies aimed at examining the RSA response of MSD417 and the MSD population to high temperature should consider applying a gradual temperature increment and a less severe treatment to mimic field conditions.

Under high temperature conditions, two parameters, SRL and RSW, were found to be significantly different between MSD417 and N61. Moreover, MSD417 had a significantly wider SPSRA than N61. Among these parameters, SPSRA are considered to be inherited traits determined during the four days at controlled temperatures, rather than by their response to high temperature. Higher SRL in MSD417 under high-temperature conditions than that in N61 is intriguing: SRL is a commonly measured parameter, but its physiological significance remains to be fully resolved **[58]**. High SRL may suggest thinner roots and a lower cost of root system construction, which requires less carbon and potentially leads to higher soil resource uptake efficiency. However, the cheaply constructed root system may have a shorter lifespan, thus it can be less efficient for long-term resource uptake **[59,60]**. The physiological significance of higher SRL in MSD417 should be examined in future studies.

The MSD417 exhibited a distinct coleorhiza morphological feature, which was larger than that of N61 at 7 days after germination (Figure 7). Coleorhiza is a sheath-like, nonvascular organ that surrounds the radicle in grass embryos **[61–63]**. Coleorhiza is established before the end of

seed development, and functions in the control of dormancy maintenance and germination through modulation of cell wall remodeling **[61]**. Upon germination, the coleorhiza expands from the caryopsis into the environment, and then the radicle emerges into the soil by rupturing the coleorhiza. In *Avena fatua* (wild oat), coleorhiza growth occurs before the growth of the radicle, and is achieved by cell expansion mainly in the longitudinal direction **[61]**. In this step, a localized expression of cell wall remodeling proteins, xyloglucan endotransglycosylases/ hydrolases, is implicated in this expansion. The tendency for longitudinal cell expansion was also observed in the present study in N61. In contrast, the transversally active expansion of coleorhiza in MSD417 suggests that cell wall remodeling may also be activated in the lateral side of the coleorhiza in this genotype. Since gene expression of cell wall remodeling proteins is regulated by plant hormones such as gibberellins and ethylene **[44,64]**, the altered coleorhiza expansion in MSD417 may involve differences in the mechanisms of action of these plant hormones.

In the present study, we developed a versatile 2D root phenotyping system and characterized a unique wide root angle trait in the wheat MSD417 genotype. The multiple synthetic derivatives (MSD) population has over 400 representative genotypes **[12]**. Analysis of their root system architecture (RSA) in a high-throughput manner in the future may lead to the discovery of new genotypes exhibiting distinct root development traits for agricultural benefits. Moreover, although previous studies have indicated that the RSA traits at the seedling stage, including rooting angle, could be a useful proxy for those of mature root systems **[7,65,66]**, verification is needed to determine whether the trait of enhanced lateral root development in MSD417 is also observed in the mature crop under field conditions. Overall, continued research on the genetic and environmental regulation of root development will contribute to a framework for improving the agricultural performance of wheat, thereby supporting the development of cultivars with improved productivity.

5. Conclusions

In this study, we successfully employed a simplified 2D-root phenotyping platform and characterized MSD417 as possessing distinct root traits compared with its recurrent parent, N61, under contrasting temperature regimes. Under control conditions, MSD417 developed a larger root system primarily as a consequence of an increased root system width, which was driven by a broader angle of the outermost pair of seminal roots, while maintaining comparable rooting depth to N61. This architectural configuration suggests that MSD417 may overcome the typical trade-off between shallow and deep soil foraging, a trait highly desirable for efficient nutrient and water capture. Furthermore, the unique transversal expansion of the coleorhiza in MSD417 may indicate potentially novel, genotype-specific mechanisms of cell wall remodeling that should be explored at the molecular level. Although high-temperature stress obscured the major morphological differences between genotypes, maintaining higher specific root length in MSD417 indicates an inherent capacity for efficient resource acquisition even under high-temperature stress. Nevertheless, to establish MSD417 as a valuable genotype for breeding programs, further validation of these traits in mature plants under field conditions is required. Ultimately, the experimental approaches presented here provide a framework for leveraging the genetic diversity of the MSD and similar populations to uncover variation in RSA.

Author Contributions: Conceptualization, S.M.M.I. and K.A.; methodology, S.M.M.I. and KA; software, S.M.M.I.; validation, S.M.M.I., I.S.A.T., and K.A.; formal analysis, S.M.M.I.; investigation, S.M.M.I.; resources,

S.M.M.I.; data curation, S.M.M.I.; writing—original draft preparation, S.M.M.I.; writing—review and editing, I.S.A.T. and K.A.; visualization, S.M.M.I. and K.A.; supervision, K.A.; project administration, K.A.; funding acquisition, K.A. All authors have read and agreed to the published version of the manuscript.

Funding: This research was funded by the Project Marginal Region Agriculture, the Arid Land Research Center, Tottori University, and the IPDRE Program, Tottori University.

Acknowledgments: We are grateful to Prof Hiroyuki Tanaka (Faculty of Agriculture, Tottori University, Tottori, Japan) and Dr Yasir Serag Alnor Gorafi (Graduate School of Agriculture, Kyoto University, Kyoto, Japan) for providing seeds of wheat cultivar Norin 61 and the MSD genotype MSD417, respectively. We thank the staff members of the Laboratory of Molecular and Cellular Biology, Faculty of Agriculture, Tottori University, for their technical support in the laboratory.

Conflicts of Interest: The authors declare no conflict of interest.

Reference

1. Erenstein O, Jaleta M, Mottaleb KA, Sonder K, Donovan J, Braun H-J. Global trends in wheat production, consumption and trade. In: Reynolds MP, Braun H-J, editors. Wheat Improvement: Food Security in a Changing Climate. Cham: Springer International Publishing; 2022. pp. 47–66. doi:10.1007/978-3-030-90673-3_4

2. Pequeno DNL, Hernández-Ochoa IM, Reynolds M, Sonder K, MoleroMilan A, Robertson RD, et al. Climate impact and adaptation to heat and drought stress of regional and global wheat production. Environ Res Lett. 2021;16: 054070. doi:10.1088/1748-9326/abd970

3. Asseng S, Ewert F, Martre P, Rötter RP, Lobell DB, Cammarano D, et al. Rising temperatures reduce global wheat production. Nat Clim Change. 2015;5: 143–147. doi:10.1038/nclimate2470

4. Farhad M, Kumar U, Tomar V, Bhati PK, Krishnan J. N, Kishowar-E-Mustarin, et al. Heat stress in wheat: a global challenge to feed billions in the current era of the changing climate. Front Sustain Food Syst. 2023;7: 1203721. doi:10.3389/fsufs.2023.1203721

5. Cope JE, Berckx F, Galinski A, Lentz J, Nagel KA, Fiorani F, et al. Precrop-treated soil influences wheat (*Triticum aestivum* L.) root system architecture and its response to drought. Front Plant Sci. 2024;15: 1389593. doi:10.3389/fpls.2024.1389593

6. Lynch JP. Harnessing root architecture to address global challenges. Plant J. 2022;109: 415–431. doi:10.1111/tpj.15560

7. Kang Y, Rambla C, Haeften SV, Fu B, Akinlade O, Potgieter AB, et al. Seminal root angle is associated with root system architecture in durum wheat. Food Energy Secur. 2024;13: e570. doi:10.1002/fes3.570

8. Lynch JP. Roots of the second green revolution. Aust J Bot. 2007;55: 493–512. doi:10.1071/BT06118

9. Ober ES, Alahmad S, Cockram J, Forestan C, Hickey LT, Kant J, et al. Wheat root systems as a breeding target for climate resilience. Theor Appl Genet. 2021;134: 1645–1662. doi:10.1007/s00122-021-03819-w

10. Elbashir AAE, Gorafi YSA, Tahir ISA, Elhashimi AMA, Abdalla MGA, Tsujimoto H. Genetic variation in heat tolerance-related traits in a population of wheat multiple synthetic derivatives. Breed Sci. 2017;67: 483–492. doi:10.1270/jsbbs.17048

11. Gorafi YSA, Kim J-S, Elbashir AAE, Tsujimoto H. A population of wheat multiple synthetic derivatives: an effective platform to explore, harness and utilize genetic diversity of *Aegilops tauschii* for wheat improvement. Theor Appl Genet. 2018;131: 1615–1626. doi:10.1007/s00122-018-3102-x

12. Gorafi YSA, Tahir ISA, Tsujimoto H. A Multiple Synthetic Derivatives population for mining *Aegilops tauschii* traits and genes in a background of common wheat. J Plant Regist. 2025;19: e20424. doi:10.1002/plr2.20424

13. Tsujimoto H, Sohail Q, Matsuoka Y. Broadening the genetic diversity of common and durum wheat for abiotic stress tolerance breeding. In: Ogihara Y, Takumi S, Handa H, editors. Advances in Wheat Genetics: From Genome to Field. Tokyo: Springer Japan; 2015. pp. 233–238. doi:10.1007/978-4-431-55675-6_25

14. Matsunaga S. Multi-omics studies of thermal response towards the development of heat-tolerant bread wheat. PhD Thesis, Tottori University. 2022. Available: https://cir.nii.ac.jp/crid/1910865335618267008

15. Johnson MG, Tingey DT, Phillips DL, Storm MJ. Advancing fine root research with minirhizotrons. Environ Exp Bot. 2001;45: 263–289. doi:10.1016/s0098-8472(01)00077-6

16. Maqbool S, Hassan MA, Xia X, York LM, Rasheed A, He Z. Root system architecture in cereals: progress, challenges and perspective. Plant J Cell Mol Biol. 2022;110: 23–42. doi:10.1111/tpj.15669

17. Trachsel S, Kaeppler SM, Brown KM, Lynch JP. Shovelomics: high throughput phenotyping of maize (*Zea mays* L.) root architecture in the field. Plant Soil. 2011;341: 75–87. doi:10.1007/s11104-010-0623-8

18. Wasson AP, Rebetzke GJ, Kirkegaard JA, Christopher J, Richards RA, Watt M. Soil coring at multiple field environments can directly quantify variation in deep root traits to select wheat genotypes for breeding. J Exp Bot. 2014;65: 6231–6249. doi:10.1093/jxb/eru250

19. Poorter H, Fiorani F, Pieruschka R, Wojciechowski T, van der Putten WH, Kleyer M, et al. Pampered inside, pestered outside? Differences and similarities between plants growing in controlled conditions and in the field. New Phytol. 2016;212: 838–855. doi:10.1111/nph.14243

20. Böhm W. Methods of studying root systems. Berlin, Heidelberg: Springer; 1979. doi:10.1007/978-3-642-67282-8

21. Neumann G, George TS, Plassard C. Strategies and methods for studying the rhizosphere—the plant science toolbox. Plant Soil. 2009;321: 431–456. doi:10.1007/s11104-009-9953-9

22. Schuurman JJ, Goedewaagen MAJ. Methods for the examination of root systems and roots: methods in use at the institute for soil fertility for eco-morphological root investigations. 2. ed. Methods for the examination of root systems and roots: methods in use at the Institute for Soil Fertility for eco-morphological root investigations. Wageningen: Centre for Agricultural Publ. and Documentation; 1971.

23. Richard CA, Hickey LT, Fletcher S, Jennings R, Chenu K, Christopher JT. High-throughput phenotyping of seminal root traits in wheat. Plant Methods. 2015;11: 13. doi:10.1186/s13007-015-0055-9

24. Gioia T, Galinski A, Lenz H, Müller C, Lentz J, Heinz K, et al. GrowScreen-PaGe, a non-invasive, high-throughput phenotyping system based on germination paper to quantify crop phenotypic diversity and plasticity of root traits under varying nutrient supply. Funct Plant Biol FPB. 2016;44: 76–93. doi:10.1071/FP16128

25. Nagel KA, Lenz H, Kastenholz B, Gilmer F, Averesch A, Putz A, et al. The platform GrowScreen-agar enables identification of phenotypic diversity in root and shoot growth traits of agar grown plants. Plant Methods. 2020;16: 89. doi:10.1186/s13007-020-00631-3

26. Nagel KA, Putz A, Gilmer F, Heinz K, Fischbach A, Pfeifer J, et al. GROWSCREEN-Rhizo is a novel phenotyping robot enabling simultaneous measurements of root and shoot growth for plants grown in soil-filled rhizotrons. Funct Plant Biol. 2012;39: 891–904. doi:10.1071/FP12023

27. Rellán-Álvarez R, Lobet G, Lindner H, Pradier P-L, Sebastian J, Yee M-C, et al. GLO-Roots: an imaging platform enabling multidimensional characterization of soil-grown root systems. Harrison MJ, editor. eLife. 2015;4: e07597. doi:10.7554/eLife.07597

28. Chen Y, Palta J, Prasad PVV, Siddique KHM. Phenotypic variability in bread wheat root systems at the early vegetative stage. BMC Plant Biol. 2020;20: 185. doi:10.1186/s12870-020-02390-8

29. Shorinola O, Kaye R, Golan G, Peleg Z, Kepinski S, Uauy C. Genetic screening for mutants with altered seminal root numbers in hexaploid wheat using a high-throughput root phenotyping platform. G3 GenesGenomesGenetics. 2019;9: 2799–2809. doi:10.1534/g3.119.400537

30. Lobet G, Pagès L, Draye X. A novel image-analysis toolbox enabling quantitative analysis of root system architecture. Plant Physiol. 2011;157: 29–39. doi:10.1104/pp.111.179895

31. Emam AII, Kamal NM, Gorafi YSA, Tahir ISA, Balla MY, Tsujimoto H, et al. Enriched grain minerals in Aegilops tauschii-derived common wheat population under heat-stress environments. Sci Rep. 2025;15: 5624. doi:10.1038/s41598-025-89144-4

32. Emam AII, Tahir ISA, Kamal NM, Gorafi YSA, Tsujimoto H, Ishii T. Genetic variation and genome-wide association analysis of nitrogen use efficiency-related traits under combined heat and nitrogen-deficient stress in an Aegilops tauschii-derived wheat population. Front Plant Sci. 2025;16. doi:10.3389/fpls.2025.1621916

33. Itam MO, Gorafi YSA, Tahir ISA, Tsujimoto H. Genetic variation in drought resilience-related traits among wheat multiple synthetic derivative lines: insights for climate resilience breeding. Breed Sci. 2021;71: 435–443. doi:10.1270/jsbbs.20162

34. Mohamed IES, Oe H, Kamal NM, Mustafa HM, Gorafi YSA, Tahir ISA, et al. Enhancing Wheat Flour Quality Through Introgression of High-Molecular-Weight Glutenin Subunits From Aegilops tauschii Accessions. Front Sustain Food Syst. 2022;6. doi:10.3389/fsufs.2022.887795

35. Rich SM, Christopher J, Richards R, Watt M. Root phenotypes of young wheat plants grown in controlled environments show inconsistent correlation with mature root traits in the field. J Exp Bot. 2020;71: 4751–4762. doi:10.1093/jxb/eraa201

36. Kirschner GK, Hochholdinger F, Salvi S, Bennett MJ, Huang G, Bhosale RA. Genetic regulation of the root angle in cereals. Trends Plant Sci. 2024;29: 814–822. doi:10.1016/j.tplants.2024.01.008

37. Mano Y, Omori F. Breeding for flooding tolerant maize using "teosinte" as a germplasm resource. Plant Root. 2007;1: 17–21. doi:10.3117/plantroot.1.17

38. Huang G, Liang W, Sturrock CJ, Pandey BK, Giri J, Mairhofer S, et al. Rice actin binding protein RMD controls crown root angle in response to external phosphate. Nat Commun. 2018;9: 2346. doi:10.1038/s41467-018-04710-x

39. Kitomi Y, Hanzawa E, Kuya N, Inoue H, Hara N, Kawai S, et al. Root angle modifications by the DRO1 homolog improve rice yields in saline paddy fields. Proc Natl Acad Sci. 2020;117: 21242–21250. doi:10.1073/pnas.2005911117

40. Oo AZ, Tsujimoto Y, Mukai M, Nishigaki T, Takai T, Uga Y. Synergy between a shallow root system with a DRO1 homologue and localized P application improves P uptake of lowland rice. Sci Rep. 2021;11: 9484. doi:10.1038/s41598-021-89129-z

41. Uga Y, Sugimoto K, Ogawa S, Rane J, Ishitani M, Hara N, et al. Control of root system architecture by DEEPER ROOTING 1 increases rice yield under drought conditions. Nat Genet. 2013;45: 1097–1102. doi:10.1038/ng.2725

42. Bodner G, Loiskandl W, Hartl W, Erhart E, Sobotik M. Characterization of cover crop rooting types from integration of rhizobox imaging and root atlas information. Plants. 2019;8: 514. doi:10.3390/plants8110514

43. Rangarajan H, Lynch JP. A comparative analysis of quantitative metrics of root architecture. Plant Phenomics. 2021;2021: 6953197. doi:10.34133/2021/6953197

44. Calleja-Cabrera J, Boter M, Oñate-Sánchez L, Pernas M. Root growth adaptation to climate change in crops. Front Plant Sci. 2020;11: 544. doi:10.3389/fpls.2020.00544

45. Huang BR, Taylor HM, McMichael BL. Effects of temperature on the development of metaxylem in primary wheat roots and its hydraulic consequence. Ann Bot. 1991;67: 163–166. doi:10.1093/oxfordjournals.aob.a088115

46. Huang B-R, Taylor HM, McMichael BL. Growth and development of seminal and crown roots of wheat seedlings as affected by temperature. Environ Exp Bot. 1991;31: 471–477. doi:10.1016/0098-8472(91)90046-Q

47. Morales D, Rodríguez P, Dell'Amico J, Nicolás E, Torrecillas A, Sánchez-Blanco MJ. High-temperature preconditioning and thermal shock imposition affects water relations, gas exchange and root hydraulic conductivity in tomato. Biol Plant. 2003;47: 203–208. doi:10.1023/B:BIOP.0000022252.70836.fc

48. Pardales JR, Bañoc DM, Yamauchi A, lijima M, Kono Y. Root system development of cassava and sweetpotato during early growth stage as affected by high root zone temperature. Plant Prod Sci. 1999;2: 247–251. doi:10.1626/pps.2.247

49. Gupta NK, Agarwal S, Agarwal VP, Nathawat NS, Gupta S, Singh G. Effect of short-term heat stress on growth, physiology and antioxidative defence system in wheat seedlings. Acta Physiol Plant. 2013;35: 1837–1842. doi:10.1007/s11738-013-1221-1

50. Iglesias-Acosta M, Martínez-Ballesta MC, Teruel JA, Carvajal M. The response of broccoli plants to high temperature and possible role of root aquaporins. Environ Exp Bot. 2010;68: 83–90. doi:10.1016/j.envexpbot.2009.10.007

51. Ionenko IF, Anisimov AV, Dautova NR. Effect of temperature on water transport through aquaporins. Biol Plant. 2010;54: 488–494. doi:10.1007/s10535-010-0086-z

52. Howell SH. Endoplasmic reticulum stress responses in plants. Annu Rev Plant Biol. 2013;64: 477–499. doi:10.1146/annurev-arplant-050312-120053

53. Vu LD, Gevaert K, De Smet I. Feeling the heat: searching for plant thermosensors. Trends Plant Sci. 2019;24: 210–219. doi:10.1016/j.tplants.2018.11.004

54. Savicka M, Škute N. Effects of high temperature on malondialdehyde content, superoxide production and growth changes in wheat seedlings (*Triticum aestivum* L.). Ekologija. 2010;56: 26–33. doi:10.2478/v10055-010-0004-x

55. Heckathorn SA, Giri A, Mishra S, Bista D. Heat stress and roots. Climate Change and Plant Abiotic Stress Tolerance. John Wiley & Sons, Ltd; 2013. pp. 109–136. doi:10.1002/9783527675265.ch05

56. Joshi M, Fogelman E, Belausov E, Ginzberg I. Potato root system development and factors that determine its architecture. J Plant Physiol. 2016;205: 113–123. doi:10.1016/j.jplph.2016.08.014

57. Sattelmacher B, Marschner H, Kühne R. Effects of the temperature of the rooting zone on the growth and development of roots of potato (*Solanum tuberosum*). Ann Bot. 1990;65: 27–36. doi:10.1093/oxfordjournals.aob.a087903

58. Freschet GT, Roumet C, Comas LH, Weemstra M, Bengough AG, Rewald B, et al. Root traits as drivers of plant and ecosystem functioning: current understanding, pitfalls and future research needs. New Phytol. 2021;232: 1123–1158. doi:10.1111/nph.17072

59. Ryser P. The importance of tissue density for growth and life span of leaves and roots: a comparison of five ecologically contrasting grasses. Funct Ecol. 1996;10: 717–723. doi:10.2307/2390506

60. Weemstra M, Kiorapostolou N, van Ruijven J, Mommer L, de Vries J, Sterck F. The role of fine-root mass, specific root length and life span in tree performance: A whole-tree exploration. Funct Ecol. 2020;34: 575–585. doi:10.1111/1365-2435.13520

61. Holloway T, Steinbrecher T, Pérez M, Seville A, Stock D, Nakabayashi K, et al. Coleorhiza-enforced seed dormancy: a novel mechanism to control germination in grasses. New Phytol. 2021;229: 2179–2191. doi:10.1111/nph.16948

62. Venglat P, Vijayan P, Sharbel TF, Rahman A, Tanino K. Phytomers, collet and founder cells: a "universal" plant embryonic body plan from a developmental, molecular, and evolutionary perspective. Front Plant Sci. 2025;16: 1521527. doi:10.3389/fpls.2025.1521527

63. Viana WG, Scharwies JD, Dinneny JR. Deconstructing the root system of grasses through an exploration of development, anatomy and function. Plant Cell Environ. 2022;45: 602–619. doi:10.1111/pce.14270

64. Ruduś I, Cembrowska-Lech D, Jaworska A, Kępczyński J. Involvement of ethylene biosynthesis and perception during germination of dormant *Avena fatua* L. caryopses induced by KAR1 or GA3. Planta. 2019;249: 719–738. doi:10.1007/s00425-018-3032-5

65. Alahmad S, El Hassouni K, Bassi FM, Dinglasan E, Youssef C, Quarry G, et al. A major root architecture QTL responding to water limitation in durum wheat. Front Plant Sci. 2019;10. doi:10.3389/fpls.2019.00436

66. Maccaferri M, El-Feki W, Nazemi G, Salvi S, Canè MA, Colalongo MC, et al. Prioritizing quantitative trait loci for root system architecture in tetraploid wheat. J Exp Bot. 2016;67: 1161–1178. doi:10.1093/jxb/erw039